Study on the Preparation of Nanocellulose Powder and Its Formation Mechanism

Zirui zhu (zhu67201457@163.com)
Qilu University of Technology
Wenbo Wang
Qilu University of Technology
Xiaohui Wang
Qilu University of Technology
Xin Zhao
Qilu University of Technology
Nannan Xia
Qilu University of Technology
Fangong Kong
Qilu University of Technology
Shoujuan Wang
Qilu University of Technology https://orcid.org/0000-0003-3357-5188

Research Article

Keywords: CNC preparation, re-dispersible CNC powder, purification process after sulfuric acid hydrolysis, mechanism of CNC powder formation

Posted Date: February 23rd, 2021

DOI: https://doi.org/10.21203/rs.3.rs-231182/v1

Version of Record: A version of this preprint was published at Cellulose on August 22nd, 2021. See the published version at https://doi.org/10.1007/s10570-021-04123-y.

Abstract

Nanocellulose is a kind of cellulose based nano material with fantastic properties and numerous potential applications. However, due to the fact that nanocellulose exhibits colloidal properties when its concentration is high, the drying of nanocellulose has always been an urgent problem to be solved. To address this problem, the precipitation and drying mechanism of cellulose nanocrystal (CNC), one of the most common types of nanocellulose, was studied in this paper. The CNC was precipitated from the aqueous suspension by salting out to avoid the CNC colloidal state when concentrated in water. The obtained CNC precipitation with a small amount of water and the actively added electrolyte was dehydrated and purified by solvent displacement with volatile organic. Then CNC powder can be taken shape by drying the mixture of CNC and organic solvent with different drying methods. The mechanism of CNC precipitation from aqueous suspension and CNC powder formation from volatile organic solvent was studied. After comprehensive consideration, a method for preparing re-dispersible CNC powder was established, and the properties of this powder were studied, that provided a solution for the industrial preparation and application of nanocellulose.

1. Introduction

Cellulose, the oldest natural polymer and the most abundant renewable resource on earth, is mainly derived from woods, bamboos, cottons, etc. (Moon et al. 2011). Nanocellulose, as a source of cellulose-based nanomaterial, exhibits better performance than traditional cellulose, such as nano-scale effect (Dufresne 2013), high surface area (Phanthong et al. 2018), outstanding mechanical strength (Nystrom et al. 2018) and high surface activity (Yang et al. 2017), etc. Recent years, with the further development of research, nanocellulose is now widely applied in biomedicine (DeLoid et al. 2018; Salimi et al. 2019), nanocomposite materials (Liu et al. 2010; Vollick et al. 2017), aerospace (Kargarzadeh et al. 2015), and environmental areas, etc. (Abouzeid et al. 2019; Kong et al. 2018; Korhonen et al. 2011). Cellulose Nanocrystal (CNC) is one of the most common types of nanocellulose which is mainly prepared by acid hydrolysis method. Normally, CNC is stored in the form of aqueous suspension due to the large number of hydrophilic groups on its surface (Sinquefield et al. 2020). However, CNC aqueous suspension tends to transform into gel state when its concentration exceeds a certain range which limits the further increase of its concentration (Peng et al. 2011). Therefore, CNC is mainly stored, transported and used in the form of low-concentration aqueous suspension (0.1-10w%) that greatly limits its industrial application (Wang et al. 2019b). Thus, the effective drying of CNC suspension is an urgent problem to be solved.

To achieve convenient storage and transportation of CNC, not only CNC must be effectively dried, but the dried CNC can be redispersed in water. Ways to improve CNC powder re-dispersion property mainly include chemical modification on CNC surface and changing the drying method of CNC suspension (Huang et al. 2020). Chemical modification is considered as an effective method to improve CNC dispersibility (Shang et al. 2019). Velásquez-Cock, J., et al. used maltodextrin (MDX), which was a capping agent, to avoid irreversible agglomeration during CNF (cellulose nanofiber) powder formation process (Velásquez-Cock et al. 2018). Liu et al. found that, when the grafting amount of PMMA on CNC

was higher than 70%, the CNC dispersible powder can be successfully prepared (Liu et al. 2020). Zhang et al. also reported a new method to prepare dispersible CNF powder by modifying CNF with phenyl trimethoxy silane (PTS), which showed excellent dispersibility in water (Zhang et al. 2019). All of the above modification methods can obtain dispersible nanocellulose powder. However, the CNC's surface functional groups or chemical structures were changed during these chemical treatments. Importantly, the employment of toxic reagents would be harmful to the environment.

Another way to prepare nanocellulose powder is to change the drying method of its aqueous suspension. The drying methods of nanocellulose usually include oven drying, freeze-drying, spray drying, and supercritical CO_2 drying (George and Montemagno 2017; Posada et al. 2020; Tsioptsias et al. 2008; Zheng and Fu 2019). Oven drying is a simple and economical way to obtain dried nanocellulose. However, the fibers of nanocellulose will become cross-linked (Uetani et al. 2018) due to the large number of hydrogen bonds on its surface which cause the nanocellulose to dry into membranes (Beck et al. 2012). Freeze-drying is a common method for preparing nanocellulose powder (Gray 2016; Varshosaz et al. 2012). But it still cannot obtain nanocellulose powder when the concentration of nanocellulose is higher than 0.5% (Han et al. 2013). Meanwhile, higher concentration CNC in the freeze drying will lead to the formation of a large number of hydrogen bonds between fibers, resulting in irreversible agglomeration of the fibers (Chen et al. 2019). Meanwhile, low concentration of nanocellulose can take a long time by freeze-drying (3–5 days) (Martinez Avila et al. 2015), which is uneconomical. Up to now, nanocellulose powder preparation by freeze-drying is only suitable for laboratory.

Spray drying and supercritical CO_2 drying can also prepare nanocellulose powder (Volk et al. 2015). However, expensive equipment, high operating costs, and low powder yield severely limit its large-scale production (Lee et al. 2013). The above existing problems restrict the promotion and application of nanocellulose which exhibit excellent performance. In order to make effective use of nanocellulose, we have done a lot of work. For example, we used ammonium bicarbonate in the purification process of nanocellulose after acid hydrolysis, which avoided the use of expensive and inefficient dialysis membranes. After homogenization, high concentration aqueous nanocellulose suspensions can be directly prepared (Wang et al. 2018). This process not only cut down the cost of CNC preparation, but also further reduced the preparation time drastically.

In this contribution, CNC containing impurities can be simply prepared by homogenizing the fiber components which were preliminary purified by centrifugation after obtaining from the dissolving pulp degradation with acid hydrolysis. After CNC was precipitated from the aqueous suspension by salting out, a volatile organic solvent such as ethanol was used to replace the water in the precipitation, and the actively added electrolyte can also be dissolved out at the same time. Then, the obtained CNC and organic solvent mixture can be precipitated and dried into pure CNC powder by different evaporation methods. The specific experiment process was that cellulose was hydrolyzed by sulfuric acid (56wt% acid concentration at 55°C for 60 min). After initial centrifugation, the hydrolysate was neutralized with sodium hydroxide. The neutral hydrolysate was homogenized 5 times under the pressure of 20,000 psi by a micro jet nano homogenizer. We chose three kinds of electrolytes, potassium acetate, copper chloride,

and ferric chloride, to precipitate CNC from the homogenized suspension by centrifugation with the purpose of removing impurities, respectively. After a few centrifuges, we got a CNC suspension containing only the actively added electrolyte as impurity. This portion of the electrolyte was removed by centrifugal replacement with a volatile organic solvent, such as ethanol. Then, pure CNC in organic solvent without any electrolytes can be prepared. After the organic solvent was removed by rotary evaporation or other evaporation methods, CNC powder can be obtained, finally.

This work opens the door to a new technology. A feasible and convenient method for the production of pure nanocellulose powder is proposed. In the following discussion, we explored the influence of the agglomeration between the actively added electrolytes (concentration, valence) and CNC. After studying the mechanism that they bind to each other, potassium acetate was considered as the optimal electrolyte in this paper. The precipitation and formation mechanism of CNC powder was proved by studying the types and strength of the force between CNC and different dispersants during evaporation. In this section, we also noticed that the steric hindrance of dispersant had a significant influence on the formation of CNC powder. Large steric hindrance can effectively avoid the combination of hydrogen bonds between CNCs, thereby further providing possibility for the preparation of CNC powder. In view of the successful preparation of CNC powder in this paper, we hope that it can facilitate the large-scale preparation, transportation, application of nanocellulose, and also can provides a solution for the industrial production and utilization of nanocellulose.

2. Experimental

2.1. Materials and reagents

Hardwood bleached dissolving pulp was obtained from Shan Dong Sun Paper Industry Joint Stock Co., Ltd. Potassium acetate, Copper chloride, Ferric chloride, and 1.2-Propylene glycol were purchased from Shanghai Maclean Biochemical Co., Ltd. Methanol, Ethanol, N-propanol, N-butanol were produced by Tianjin Fuyu Fine Chemical Co., Ltd. All these chemicals of reagent grade were used as received without further treatment. Deionized water was used in all experiments.

2.2. Preparation of CNC powders

Hardwood bleached dissolving pulp (20g, oven dry) was added into 160ml sulfuric acid (56, 59, 61, 64wt%) in a three-necked round-bottom flask. The hydrolysis was stirred by using an electrical agitator for 60 min at 55°C. The gained suspensions were washed two times with deionized water by centrifugation (4000rpm, 10min), then NaOH was added until the pH was neutral and continued centrifugation. After centrifugation, these suspensions were homogenized by high-pressure homogenization (pressure of 20,000 psi) for 5 times. After that, we added potassium acetate to the homogenized CNC to remove impurities by centrifugation. Then, ethanol was added to the precipitate to remove the potassium acetate (electrolyte content can be measured by conductivity). Finally, the CNC powder was obtained by oven drying or rotary evaporating the CNC-organic precipitation.

2.3. Analytical methods

2.3.1. Fourier-transformed infrared spectra (FT-IR) analysis

The samples after treatment were analyzed with Fourier transform Infrared (FT-IR) spectroscopy (Bruker Tensor 37, Germany) with 4000 cm^{-1} to 400 cm^{-1}.

2.3.2. Stability analyzer analysis

The stability of the purified CNC aqueous suspension was analyzed by LUMisizer (Germany) at a centrifugal speed of 3000 rpm and a temperature of 25°C.

2.3.3. AFG particle charge titrator analysis

AFG particle charge titrator (Germany) is used to determine the surface charge of different states of CNC (before and after purification). The cation titrant is Polyelectrolyte sol.

2.3.4. Scanning electron microscopy (SEM)

Scanning electron microscopy (SEM) was done with Hitachi Regulus8220 (Japan). All samples need to be sprayed with gold before testing.

2.3.5. Thermogravimetric analysis (TGA)

Thermal properties of CNC powder were studied by thermogravimetric analysis (TGA) (Q50, USA) under a nitrogen atmosphere with an alumina sample pan. The sample was heated at 10°C/min from room temperature to 700°C.

2.3.6. X-ray diffraction (XRD) analysis

X-ray diffraction patterns of the cellulose materials were determined using an X-ray diffractometer (Japanese Science SE) equipment with Cu Kα radiation in the 2θ range of 5 – 80°. The crystallinity index of cellulose materials was calculated according to the empirical method developed by Segal et al. (L. Segal et al. 1959).

$$\mathrm{CrI} = \frac{I_{002} - I_{am}}{I_{002}} \times 100\%$$

I002 is the intensity of the lattice diffraction peak, Iam is the peak intensity of the amorphous region. A diffraction angle of around 2θ = 22.5° was the peak for plane (002), and the lowest intensity at a diffraction angle of around 2θ = 18.0° was measured as the amorphous part.

2.3.7. Atomic force microscopy (AFM)

Atomic force microscopy was performed by Multimode 8 (Germany) for specimen deposited on freshly cleaved mica, CNC concentration is 0.001%.

3. Results And Discussion

3.1. Study on the combination of CNC with different electrolytes

Generally, long time-consuming is an unavoidable problem in the process of preparing CNC by sulfuric acid hydrolysis. The main reason is that during centrifugal purification process, CNC is difficult to precipitate due to its light weight (Wang et al. 2019a) and high surface charge density (Abitbol et al. 2018), which make it difficult to remove impurities from CNC aqueous suspension. Normally, scientists use dialysis to purify CNC after sulfuric acid hydrolysis (Dong et al. 2016; Kim et al. 2016). The advantage of dialysis is that it can obtain pure CNC. However, the dialysis process is expensive and time-consuming (Tang et al. 2013; Zhang et al. 2020), which greatly hinders the efficient preparation of CNC. Some researchers found that adding a positively charged electrolyte in CNC dispersion can neutralize the negative charge on its surface (Fall et al. 2011; Fukuzumi et al. 2014). It would reduce the repulsive force between CNCs, and destroy the stability of CNC suspension system based on DLVO theory (Boluk et al. 2012; Phan-Xuan et al. 2016). Therefore, here, we propose a new method to prepare CNC powder. The process is adding an electrolyte to CNC aqueous suspension during the centrifugal purification. After centrifugation, the CNC-electrolyte precipitate is dispersed in a specific organic solvent to remove the actively added electrolyte to gain the CNC-organic solvent mixture. Then, CNC powder can be obtained by oven drying or rotary evaporating this mixture. The preparation process is shown in Fig. 1(a). By comparison, we find that the new method in Fig. 1(a) only needs several hours. However, the preparation of traditional CNC suspension needs 2–7 days (Cranston and Gray 2006). What's more, the new method can further prepare re-dispersible CNC powder, direct.

After preliminary attempts and analysis, we found that successful preparation of CNC powder requires an effective pairing of electrolyte and solvent. The basic conditions are as follows: (1) the addition of electrolytes can cause CNC suspension to precipitate during centrifugation; (2) the electrolyte has a good solubility in the matched solvent; (3) the solvent needs to be miscible with water which cause the electrolyte to be removed from water to solvent; (4) the solvent should be easy to volatilize. Based on the above considerations, we chose ethanol as solvent and CH_3COOK, $CuCl_2$, and $FeCl_3$ as electrolytes in this paper. The following steps were used to study their attribute on the preparation of CNC powder. First, we investigated the agglomeration ability of CNC with CH_3COOK, $CuCl_2$, and $FeCl_3$, respectively. As shown in Fig. S1, we added different concentrations of electrolytes (CH_3COOK, $CuCl_2$, and $FeCl_3$) to CNC aqueous suspension (0.5%), then mixed well. Finally, we could obtain CNC-electrolyte precipitates after centrifuging the mixtures above, respectively.

In this test, we found that when adding different valence electrolytes in CNC suspension, the precipitate formed by high-valent electrolytes such as $CuCl_2$ and $FeCl_3$ was difficult to re-disperse in water which made it hardly to remove impurity ions in subsequent purification process. The probable reason for this phenomenon is that different valence ions have different agglomeration capabilities with CNC. High-valent ions (Cu^{2+}, Fe^{3+}) may have a strong agglomeration ability with CNC. Interestingly, in follow-up study, we verified the above conjecture in a specific experiment. By observing the tightness of CNC precipitate with different valence ions, we found that a few high-valent electrolytes can easily cause CNC precipitation.

To gain a better understanding of the above finding, we have carried out a specific investigation. Different amounts of $CuCl_2$ and $FeCl_3$ (0.2%, 0.1%, 0.05%, 0.02%) were mixed with CNC aqueous suspension and centrifuged. Then CNC with electrolyte was centrifugal several times, and the precipitates after each centrifugation were dispersed in a large amount of deionized water. In this test, only precipitate generated by adding 0.05% $CuCl_2$ or 0.02% $FeCl_3$ would not continue to produce precipitation during next centrifugation as shown in Fig. 1(b). The above experiment verifies our suppose that various valence electrolytes have a threshold value for agglomeration ability with CNC (Lyklema 2013). When it is less than this value, CNC with electrolyte do not produce precipitation after centrifugation. On the contrary, it can increase the density of precipitation, which bring more difficulties to subsequent experiments. What's more, we further studied the minimum amounts of various electrolytes which can cause CNC precipitate and the results are shown in Fig. S2.

To gain more insight into the influence of different valence electrolytes on CNC agglomeration, we added $CuCl_2$ and FeCl3 to 0.5% CNC aqueous suspension, respectively. Then dispersants containing CNC and electrolyte were centrifuged. The precipitate after centrifugation was purified with ethanol for 4 times. In addition, we conducted conductivity tests on each dispersed CNC aqueous to detect its metal ion content. The results are shown in Fig. 2(c). As can be seen, the color of CNC precipitate (yellow or light blue) obtained in the above experiment (conductivity no longer changes) was different from pure CNC precipitate (milky white). This difference indicated that CNC precipitate prepared with high-valent ions was hardly to purify. To explain this, we postulated that CNC may be complex with high-valent electrolytes (such as Cu^{2+}, Fe^{3+}). Thus, we dispersed the precipitate in deionized water. Then, a small amount of sulfuric acid and potassium acetate were added to CNC redispersion and centrifuged. The color of new precipitate had changed to white as shown in Fig. 2(c). The reason may be that, strong acid causes the bond between CNC and electrolytes to break. As a result, electrolyte ions can be re-dissolved in the solvent and the CNC precipitate can recover to its original color.

3.1.1. FT-IR spectra analysis

The bond between electrolyte and CNC we mentioned above may be a coordination bond formed by metal cation in electrolyte and hydroxyl group on CNC (Wu and Brodbelt 1994). Then, to verify the above suppose, we added different valence electrolytes into CNC aqueous suspension. After that, the CNC with

electrolyte was stirred evenly, and dried. The dried samples were analyzed by Fourier transform Infrared (FT-IR) spectrum. The infrared spectra of all samples are shown in Fig. 2(a). All samples have strong absorption peaks at 3440, 2890, 1640, and 1430 cm^{-1}. Among them, the absorption bond at about 3440 cm^{-1} is related to the stretching vibration of O-H (Phanthong et al. 2017a), the peak at around 2900 cm^{-1} is corresponding to the C – H stretching vibration (Phanthong et al. 2017b). The absorption band at about 1430 cm^{-1} results from the symmetric CH2 bending vibration (Squinca et al. 2020). Since electrolytes only affect the strength of hydroxyl group and do not react with other functional groups, the CH_2 peak is set as internal standard peak. Through the ratio of peak area OH to CH_2 to determine intensity change trend of the OH peak. The results are shown in Fig. 2(b). As content of Cu^{2+} and Fe^{3+} gradually increased, the ratio of the peak area of OH to CH_2 will drop significantly, which shows that intensity of the hydroxyl peak is continuously decreasing. However, the addition of K^+ do not cause this change which shows that CH_3COOK is difficult to produce complex with CNC during mixing process.

3.1.2. Particle charge titrator analysis

Meanwhile, we have conducted surface charge tests on CNC at different stages. We added 0.3% CH_3COOK, 0.03% $CuCl_2$ and 0.01% $FeCl_3$ to 0.5% CNC aqueous suspension, respectively. Before and after purification, surface charge of CNC-electrolyte has been measured and shown in Fig. 2(c). From the figures, we can notice that surface charge of CNC added with high-valent electrolyte dropped sharply compared with monovalent electrolyte. And only the surface charge of CNC-K after purification is close to its original value. Surface charge of CNC purified by adding $CuCl_2$ and $FeCl_3$ is much lower than that of original CNC. This also illustrate that CNC's hydroxyl group may complex with Cu^{2+} and Fe^{3+}.

3.1.3. Stability analyzer analysis

In addition to the methods above, the state of CNC complexes with high-valent electrolytes were also confirmed by Stability Analyzer. Here, we added some electrolytes (CH_3COOK, $CuCl_2$, $FeCl_3$) to CNC suspension, and then purified it with ethanol until the conductivity no longer changed. Finally. the precipitate was dispersed in deionized water and tested. From Fig. 2(d), it can be seen that transmittance of three CNC suspensions is similar, about 80%. This is because most electrolytes have been removed in the centrifugal purification. In Fig. 2(e), we can see that the integral transmittance of CNC-K was higher than others. This is most likely due to the complexation of Cu^{2+} or Fe^{3+} with CNC, which reduces the transmission. Thereby the light transmittance of CNC-Cu and CNC-Fe is slightly lower than that of CNC-K.

By analyzing the three experiments above, we found that high-valent electrolytes could form complex with CNC that influence the stability of CNC dispersion. Thus, high-valent electrolytes such as $FeCl_3$ and $CuCl_2$ were not suitable to be used in this paper, although only a small amount of thus electrolytes can cause CNC precipitation. Consequently, the CH_3COOK was selected to agglomerate CNC in subsequent experiments.

3.2. The influence of different dispersants on CNC drying

On the basis of the analysis above, we found the optimum electrolyte and corresponding solvent for preparing CNC. Furthermore, when we tried to dry the new CNC with ethanol by rotary evaporation, we unexpectedly discovered that the nanocellulose suspension did not exhibit a gel state during the concentration process. After continuing to dry, the nanocellulose powder is obtained. In order to study the formation mechanism, we conducted the following series of experiments

Upon drying process, CNC can get diverse drying morphology in different dispersants, which play a key role in CNC drying process. Generally, CNC is dried in water to form a film. However, in the above experiment, the CNC powder can be obtained by drying with ethanol. We consider that the biggest difference between ethanol and water (as a dispersant) is that only one hydrogen bond can be formed between ethanol and CNC, while water can form two. Different number of hydrogen bonds formed between dispersant and CNC may change the dry form of CNC. In order to test the influence of dispersant on CNC dry form, we tested several other dispersions such as methanol, tetrahydrofuran, acetone and 1,2-Propylene glycol. First, we added electrolyte to make CNC precipitate, then used the above organic dispersants to remove electrolyte salts by centrifugation, respectively. Finally, the dried CNC could be obtained by drying these CNC-organic solvent mixtures. After that, we observed the morphology of the dried CNC. The results are shown in Fig. 3(a). We can notice that CNC powder can be obtained with dispersions (such as methanol, ethanol, tetrahydrofuran, and acetone) which can form a single hydrogen bond with CNC. On the contrary, the dispersants (water,1.2-Propylene glycol) that form double hydrogen bonds with CNC formed CNC film after drying.

After the above analysis, we postulate that, dispersant such as water or 1.2-Propylene glycol may generate multiple hydrogen bonds with adjacent CNCs. As drying proceeds, the CNC on both sides of dispersant will be aggregated by hydrogen bonding, resulting in the "zipper effect" (Zhou et al. 2019). Therefore, a large number of hydrogen bonds cross-links between CNCs are generated. On the contrary, dispersants (methanol, ethanol, tetrahydrofuran and acetone) that can form a single hydrogen bond with CNC will not cause "zipper effect". What’s more, Fig. 3(b) shows the formation of different hydrogen bonds between above dispersant and CNC. It illustrates that CNC can be pulled to any position in dispersants that form hydrogen bonds only, such as ethanol, unlike the “zipper effect” formed by CNC drying in water. Meanwhile, the different movements between fibers during CNC drying will also influence their dry forms.

In previous experiment, we also found an unexpected result, the shape of CNC powder dried by ethanol is larger than that dried by methanol, under the same conditions, as shown in Fig. 3(a). The approximate reason is that steric hindrance of dispersant has an effect on the final dry morphology of CNC. According to the perspective of steric hindrance, ethanol is larger than methanol, so CNC powder dried in methanol is finer. To gain more insight, we conducted further experiments to prove the above postulate. We used oven and rotary evaporation to dry CNC-methanol, CNC-ethanol, CNC-n-propanol, and CNC-n-butanol, respectively. The results are shown in Fig. 3(c), CNC-methanol, CNC-ethanol, and CNC-n-propanol are all bulk solids after oven drying, while the form of CNC after drying is powdery. A similar situation also occurs in rotary evaporation. Among them, CNC-methanol form a powder with big pieces, while CNC-

ethanol, CNC-n-propanol, and CNC-n-butanol all form powder with small pieces after drying. The comparison shows that the shape of the dried CNC will smaller as the steric hindrance of the dispersant increases, until it forms powder. This result is entirely consistent with our suppose. It also shows that different drying methods will cause different consequences.

To further investigate the formation mechanism of CNC powder, the powders and films prepared above were analyzed by scanning electron microscopy, and all results are shown in Fig. 4. Figure 4a and 4b show the microstructure of dried CNC which is produced by water and 1.2-Propylene glycol, showing that surface of the sample is smooth. But in Fig. 4b we can see obvious cracks between fibers, which may be caused by the large steric hindrance. Figure 4c-4f show the microstructure of dried CNC prepared with methanol, ethanol, n-propanol and n-butanol by oven drying. The results show that the surface of samples is rough and fibers are separated which are different from the previous two images. This is mainly due to the different number of hydrogen bonds formed between dispersant and CNC. It also shows that the CNC surface which is dried by methanol is relatively flat, and connections between fibers are tight. In contrast, the surface of other samples is uneven and shows many fractures due to the change of steric hindrance. This also explains why the dry form of CNC changed from bulk to powder. Figure 4g-4j show the microstructure of dried CNCs prepared with methanol, ethanol, n-propanol and n-butanol by rotary evaporation. These images also confirm this explanation. Although the dry solids are powders, the cross-linking of the fibers within the powder can be greatly reduced with the increase of steric hindrance of dispersants.

Based on the above exploration, we consider that the successful preparation of CNC powder which is dispersible needs to meet the following three conditions.

1). Hydrogen bond: The number of hydrogen bonds formed between dispersant and CNC can influence the morphology of dried CNC. After the previous analysis, we suppose that the existence of double hydrogen bonds will cause "zipper effect" between CNC during drying process. Then, CNC forms an inseparable hydrogen bonds with cross-linked network. In contrast, dispersion that form a single hydrogen bond will randomly connect CNC, and destroy this cross-linked network.

2). Surface tension: Water has a high surface tension (surface tension of water: 72.76 mN·m-1) (Kalová and Mareš 2015) which may cause CNC to be subjected to a strong tensile force when it is dried (Hanif et al. 2017). Compared with water, alcohol has a lower surface tension (methanol: 22.73 mN·m-1, Ethanol: 22.39 mN·m-1, N-propanol: 23.3 mN·m-1, N-butanol: 24.60 mN·m-1) (Basařová et al. 2019; Hu et al. 2008; Souc˘kova et al. 2008; Yue and Liu 2016), thus alcohol can only produce lower tensile force during dry process. Consequently, dispersants with low surface tension can be more effectively to dry CNC into powder morphology.

3). Steric hindrance: Steric hindrance also plays an important role in the formation of CNC powder. Dispersants with high steric hindrance are difficult to cause tight cross-linking state of CNC during the drying process. It can be proved by the above SEM images that as the steric hindrance of the dispersant increases, the distance between CNC will also increase, which can make it difficult to produce dense

hydrogen bond cross-links between CNC. Hence, the successful preparation of CNC powder also requires dispersants with large steric hindrance.

In view of the fact that CNC powder has been successfully prepared by the new method, in order to further explore its property, we compared the performance of prepared CNC powders (CNC-Ethanol, CNC-N-butanol) and CNC film (CNC-Water). Among them, CNC-Water is a CNC thin film prepared by drying CNC in water. CNC-Ethanol and CNC-N-butanol are CNC powders prepared by solvent replacement and rotary evaporation.

3.3. Thermal stability of CNC powder

The Thermogravimetric (TG) test results of all samples are shown in Fig. 5(a) and 5(b). All samples have a little weight loss (about 1–3%) at low temperature (< 100°C) is corresponding to the evaporation of water. Among them, CNC-Water curve has a significant reduction at 300°C. CNC-Ethanol and CNC-N-butanol show significant weightlessness at 220°C and 200°C, respectively, which is lower than CNC-Water. This is because that powdery CNC are loosely connected, exposing more surfaces, which may lead to lower thermal stability. At the same time, through the analysis of previous experiments, the fibers in CNC powder dried with n-butanol are relatively loosely arranged. Therefore, its decomposition temperature is lowest, about 20°C lower than CNC powder dried with ethanol. From the TG diagram, we can conclude that there is a connection between the degree of looseness of CNC powder and the steric hindrance of dispersant which supports our previous conclusions.

3.4. The crystallinity of CNC powder

Figure 5(c) and 5(d) show the XRD measurements and crystallinity of the samples. It can be seen from Fig. 5(c) that diffraction peaks appear at 16°, 22°, and 35°, and there is no double peak at the largest peak, so the prepared CNC is a typical type I cellulose crystal structure (Zhuo et al. 2017), which shows that different CNC drying forms would not affect their crystal structures. Figure 5(d) shows the crystallinity of the samples. We found that the crystallinity of these samples does not changed significantly. As a result, in this paper, different drying methods have no effect on the crystallinity of the CNC after drying (powder or film).

3.5. Dispersibility of CNC powder

Since re-dispersibility is a very important property of CNC powder, we redispersed the dry CNC powder produced with different electrolytes (CH_3COOK, $CuCl_2$, $FeCl_3$) in deionized water to obtained the CNC re-dispersions. Then, we irradiated the redispersion with a laser pointer (λ = 650nm), and examined the re-dispersibility. It can be seen from Fig. 6, three kinds of CNC redispersions are accompanied by the obvious Tyndall phenomenon which prove their colloidal-like state and nano-size. However, the powders in 6(b) and 6(c) show different colors which indicate that there is a small amount of metal ions (blue represents Cu^{2+}, yellow represents Fe^{3+}) in the powders. Meanwhile, we discover that a little precipitate was at bottom of the CNC redispersion as shown in Fig. 6(c), which also demonstrate the presence of

complexes. For better comparison, the above CNC re-dispersions were observed by Atomic Force Microscope (AFM). The result is shown in Fig. 6. AFM observation shows that fibers in CNC-K are obviously separated. On the contrary, fibers in CNC-Cu or CNC-Fe are partially agglomerated. This result is consistent with what we said and discussed earlier that CH_3COOK and ethanol are most suitable for this preparation method of CNC powder with re-dispersibility.

3.6. The yield and morphology of CNC prepared in new method

We further detect the practical application performance of the CNC prepared in this article. Here, we compared the yield and fiber morphology of the new method with the traditional method.

We adopted the new method to prepare CNC with different concentrations (56wt%, 59wt%, 61wt% and 64wt%) of sulfuric acid, respectively. Then, in purification process, we used CH_3COOK and ethanol as electrolyte and corresponding dispersant. The results are shown in Fig. 7 that the sulfuric acid concentration has a marked impact on the yield of CNC suspension. When the concentration of sulfuric acid increased from 56wt% to 64wt%, the yield of CNC dropped significantly. Among them, the highest yield reached 91.2% which produced by 56wt% sulfuric acid. The reason for this situation is that high sulfuric acid concentration will cause further acidolysis which degrade cellulose into glucose (Benini et al. 2018). And these results are similar to the published literature (Mahmud et al. 2019; Shahabi-Ghahafarrokhi et al. 2015).

The morphology of the samples observed by AFM were showed in Fig. 7. From AFM images, we can clearly see that the length of CNC will decrease while the acid concentration increases. The average length of CNC made from 56wt% sulfuric acid is 128nm, and the average length of CNC made from 59wt% sulfuric acid is 97nm, the average length of the CNC made from 61wt% sulfuric acid is 76nm, and the CNC made from 64wt% sulfuric acid has the shortest length, with an average length of 61nm. The length of prepared CNC is consistent with the results of previous research (Baek et al. 2013; Boluk et al. 2011; Jia and Liu 2019).

4. Conclusions

This paper proposed a novel method for preparing dispersible CNC powder. In the preparation process of nanocellulose, we innovatively adopted a new purification method by adding potassium acetate to the sulfuric acid hydrolysate of the dissolving pulp to remove impurity ions. Then, ethanol was used to get rid of the actively added potassium acetate to obtain concentrated pure CNC. The CNC powder was successfully produced by simple drying, finally. Then we further explored its formation mechanism by studying the number of hydrogen bonds formed between the dispersant and CNC, the surface tension and steric hindrance of the dispersant. The results showed that the above three factors would affect the final morphology of CNC after drying.

Compared with CNC film, the crystallinity of CNC powder did not change, but the thermal stability of CNC powder was decreased (about 80°C). The prepared CNC powder also has good dispersibility in water. Meanwhile, the yield and morphology of the prepared CNC powder are comparable with those of the traditional method.

The formation of CNC powder is analyzed from the microstructure level. Since the gaps between microscopic fibers in CNC powder are significantly larger than that in the CNC film, this allows the CNC powder to be dispersed in water. The production of nanocellulose powder will have a significant influence on transportation of traditional nanocellulose aqueous suspension, which can greatly reduce transportation costs.

Declarations

Acknowledgments

This work is supposed by the Natural Science Foundation of Shandong Province, China (ZR2020QE096, ZR2020MC156), National Natural Science Foundation of China (Grant No. 31971605), Shandong Key R&D Program (No.2019JZZY010407, 2019JZZY010304) and Special Foundation for National Science and Technology Basic Research Program of China (2019FY100902).

Conflict of Interest

The authors declare that they have no conflict of interest.

References

Abitbol T, Kam D, Levi-Kalisman Y, Gray DG, Shoseyov O (2018) Surface Charge Influence on the Phase Separation and Viscosity of. Cellulose Nanocrystals Langmuir 34:3925–3933. doi:10.1021/acs.langmuir.7b04127

Abouzeid RE, Khiari R, El-Wakil N, Dufresne A (2019) Current State and New Trends in the Use of Cellulose Nanomaterials for. Wastewater Treatment Biomacromolecules 20:573–597. doi:10.1021/acs.biomac.8b00839

Baek C, Hanif Z, Cho SW, Kim DI, Um SH (2013) Shape control of cellulose nanocrystals via compositional acid hydrolysis. J Biomed Nanotechnol 9:1293–1298. doi:10.1166/jbn.2013.1535

Basařová P, Kryvel Y, Crha J (2019) Bubble Rise Velocity and Surface Mobility in Aqueous Solutions of Sodium Dodecyl Sulphate and n. -Propanol Minerals 9:743. doi:10.3390/min9120743

Beck S, Bouchard J, Berry R (2012) Dispersibility in water of dried nanocrystalline. cellulose Biomacromolecules 13:1486–1494. doi:10.1021/bm300191k

Benini K, Voorwald HJC, Cioffi MOH, Rezende MC, Arantes V (2018) Preparation of nanocellulose from Imperata brasiliensis grass using Taguchi. method Carbohydr Polym 192:337–346. doi:10.1016/j.carbpol.2018.03.055

Boluk Y, Lahiji R, Zhao L, McDermott MT (2011) Suspension viscosities and shape parameter of cellulose nanocrystals (CNC). Colloids Surf A 377:297–303. doi:10.1016/j.colsurfa.2011.01.003

Boluk Y, Zhao L, Incani V (2012) Dispersions of nanocrystalline cellulose in aqueous polymer solutions: structure formation of. colloidal rods Langmuir 28:6114–6123. doi:10.1021/la2035449

Chen YM et al (2019) Anisotropic nanocellulose aerogels with ordered structures fabricated by directional freeze-drying. for fast liquid transport Cellulose 26:6653–6667. doi:10.1007/s10570-019-02557-z

Cranston ED, Gray DG (2006) Morphological Optical Characterization of Polyelectrolyte Biomacromolecules 7:2522–2530

DeLoid GM et al (2018) Reducing Intestinal Digestion and Absorption of Fat Using a Nature-Derived Biopolymer: Interference of Triglyceride Hydrolysis by Nanocellulose. ACS Nano 12:6469–6479. doi:10.1021/acsnano.8b03074

Dong S, Bortner MJ, Roman M (2016) Analysis of the sulfuric acid hydrolysis of wood pulp for cellulose nanocrystal production: A central composite design study Industrial. Crops Products 93:76–87. doi:10.1016/j.indcrop.2016.01.048

Dufresne A (2013) Nanocellulose: a new ageless bionanomaterial. Mater Today 16:220–227

Fall AB, Lindstrom SB, Sundman O, Odberg L, Wagberg L (2011) Colloidal stability of aqueous nanofibrillated. cellulose dispersions Langmuir 27:11332–11338. doi:10.1021/la201947x

Fukuzumi H, Tanaka R, Saito T, Isogai A (2014) Dispersion stability and aggregation behavior of TEMPO-oxidized cellulose nanofibrils in water as a function of. salt addition Cellulose 21:1553–1559. doi:10.1007/s10570-014-0180-z

George M, Montemagno C (2017) Estimation of the sulfur ester content of cellulose nanocrystals prepared by sulfuric acid hydrolysis: a reproducible and fast infrared method Wood. Science Technology 51:535–556. doi:10.1007/s00226-016-0885-2

Gray DG (2016) Recent Advances in Chiral Nematic Structure and Iridescent Color of Cellulose Nanocrystal Films Nanomaterials (Basel) 6:213 doi:10.3390/nano6110213

Han J, Zhou C, Wu Y, Liu F, Wu Q (2013) Self-assembling behavior of cellulose nanoparticles during freeze-drying: effect of suspension concentration, particle size, crystal structure, and. surface charge Biomacromolecules 14:1529–1540. doi:10.1021/bm4001734

Hanif Z et al (2017) Butanol-mediated oven-drying of nanocellulose with enhanced dehydration rate and aqueous re-dispersion. J Polym Res 25:191. doi:10.1007/s10965-017-1343-z

Hu SL, Lu T, Lan YR, Huang JB (2008) Surface Properties of Gemini Surfactants in Ethanol-Water Mixtures. Acta Phys-Chim Sin 24:2309–2313. doi:10.3866/pku.whxb20081227

Huang D, Wu M, Wang C, Kuga S, Huang Y (2020) Effect of Partial Dehydration on Freeze-Drying of Aqueous Nanocellulose Suspension. ACS Sustainable Chemistry Engineering 8:11389–11395. doi:10.1021/acssuschemeng.0c03688

Jia W, Liu Y (2019) Two characteristic cellulose nanocrystals (CNCs) obtained from oxalic acid and sulfuric acid. processing Cellulose 26:8351–8365. doi:10.1007/s10570-019-02690-9

Kalová J, Mareš R (2015) Reference Values of Surface Tension of Water International. Journal of Thermophysics 36:1396–1404. doi:10.1007/s10765-015-1907-2

Kargarzadeh H, Sheltami M, Ahmad R, Abdullah I, Dufresne I A (2015) Cellulose nanocrystal: A promising toughening agent for unsaturated polyester nanocomposite. Polymer 56:346–357. doi:10.1016/j.polymer.2014.11.054

Kim D-Y, Lee B-M, Koo DH, Kang P-H, Jeun J-P (2016) Preparation of nanocellulose from a kenaf core using E-beam irradiation and acid hydrolysis. Cellulose 23:3039–3049. doi:10.1007/s10570-016-1037-4

Kong W, Li Q, Li X, Su Y, Yue Q, Zhou W, Gao B (2018) Removal of copper ions from aqueous solutions by adsorption onto wheat straw cellulose-based polymeric composites. J Appl Polym Sci 135:46680. doi:10.1002/app.46680

Korhonen JT, Kettunen M, Ras RH, Ikkala O (2011) Hydrophobic nanocellulose aerogels as floating, sustainable, reusable, and recyclable oil absorbents. ACS Appl Mater Interfaces 3:1813–1816. doi:10.1021/am200475b

Segal L, Creely JJ, Martin AE Jr, Conrad CM (1959) An Empirical Method for Estimating the Degree of Crystallinity of Native Cellulose Using the X-Ray Diffractometer. Text Res J 29:786–794

Lee DJ, Jangam S, Mujumdar AS (2013) Some Recent Advances in Drying Technologies to Produce Particulate Solids Kona Powder and Particle Journal:69–83

Liu H, Liu D, Yao F, Wu Q (2010) Fabrication and properties of transparent polymethylmethacrylate/cellulose nanocrystals composites. Bioresour Technol 101:5685–5692. doi:10.1016/j.biortech.2010.02.045

Liu Y et al (2020) Air-dried porous powder of polymethyl methacrylate modified cellulose nanocrystal nanocomposite and its diverse applications Composites. Science Technology 188:107985. doi:10.1016/j.compscitech.2019.107985

Lyklema J (2013) Coagulation by multivalent counterions and the Schulze-Hardy rule. J Colloid Interface Sci 392:102–104. doi:10.1016/j.jcis.2012.09.066

Mahmud MM, Perveen A, Jahan RA, Matin MA, Wong SY, Li X, Arafat MT (2019) Preparation of different polymorphs of cellulose from different acid hydrolysis medium. Int J Biol Macromol 130:969–976. doi:10.1016/j.ijbiomac.2019.03.027

Martinez Avila H et al (2015) Novel bilayer bacterial nanocellulose scaffold supports neocartilage formation in vitro and in vivo. Biomaterials 44:122–133. doi:10.1016/j.biomaterials.2014.12.025

Moon RJ, Martini A, Nairn J, Simonsen J, Youngblood J (2011) Cellulose nanomaterials review: structure, properties and nanocomposites Chem. Soc Rev 40:3941–3994. doi:10.1039/c0cs00108b

Nystrom G, Arcari M, Adamcik J, Usov I, Mezzenga R (2018) Nanocellulose Fragmentation Mechanisms and Inversion of Chirality from the Single Particle to the Cholesteric Phase. ACS Nano 12:5141–5148. doi:10.1021/acsnano.8b00512

Peng Y, Gardner DJ, Han Y (2011) Drying cellulose nanofibrils: in search of a suitable method. Cellulose 19:91–102. doi:10.1007/s10570-011-9630-z

Phan-Xuan T, Thuresson A, Skepö M, Labrador A, Bordes R, Matic A (2016) Aggregation behavior of aqueous cellulose nanocrystals: the effect of. inorganic salts Cellulose 23:3653–3663. doi:10.1007/s10570-016-1080-1

Phanthong P, Karnjanakom S, Reubroycharoen P, Hao X, Abudula A, Guan G (2017a) A facile one-step way for extraction of nanocellulose with high yield by ball milling with. ionic liquid Cellulose 24:2083–2093. doi:10.1007/s10570-017-1238-5

Phanthong P, Karnjanakom S, Reubroycharoen P, Hao XG, Abudula A, Guan GQ (2017b) A facile one-step way for extraction of nanocellulose with high yield by ball milling with. ionic liquid Cellulose 24:2083–2093. doi:10.1007/s10570-017-1238-5

Phanthong P, Reubroycharoen P, Hao X, Xu G, Abudula A, Guan G (2018) Nanocellulose: Extraction and application. Carbon Resources Conversion 1:32–43. doi:10.1016/j.crcon.2018.05.004

Posada P et al (2020) Drying and redispersion of plant cellulose nanofibers for industrial applications:. a review Cellulose 27:10649–10670. doi:10.1007/s10570-020-03348-7

Salimi S, Sotudeh-Gharebagh R, Zarghami R, Chan SY, Yuen KH (2019) Production of Nanocellulose and Its Applications in Drug Delivery: A Critical Review. ACS Sustainable Chemistry Engineering 7:15800–15827. doi:10.1021/acssuschemeng.9b02744

Shahabi-Ghahafarrokhi I, Khodaiyan F, Mousavi M, Yousefi H (2015) Preparation and Characterization of Nanocellulose from Beer Industrial Residues Using Acid Hydrolysis/Ultrasound. Fibers Polym 16:529–

536. doi:10.1007/s12221-015-0529-4

Shang Z et al (2019) Improving dispersion stability of hydrochloric acid hydrolyzed cellulose nano-crystals. Carbohydr Polym 222:115037. doi:10.1016/j.carbpol.2019.115037

Sinquefield S, Ciesielski PN, Li K, Gardner DJ, Ozcan S Perspectives (2020) Nanocellulose Dewatering and Drying: Current State and Future. ACS Sustainable Chemistry Engineering 8:9601–9615. doi:10.1021/acssuschemeng.0c01797

Souc˘kova M, Klomfar J, tek JP (2008) < Measurement and Correlation of the Surface Tension-Temperature Relation for Methanol.pdf > J Chem Eng 53:2233–2236

Squinca P, Bilatto S, Badino AC, Farinas CS (2020) Nanocellulose Production in Future Biorefineries: An Integrated Approach Using Tailor-Made Enzymes. ACS Sustainable Chemistry Engineering 8:2277–2286. doi:10.1021/acssuschemeng.9b06790

Tang Y, Yang S, Zhang N, Zhang J (2013) Preparation and characterization of nanocrystalline cellulose via low-intensity ultrasonic-assisted sulfuric. acid hydrolysis Cellulose 21:335–346. doi:10.1007/s10570-013-0158-2

Tsioptsias C, Stefopoulos A, Kokkinomalis I, Papadopoulou L, Panayiotou C (2008) Development of micro- and nano-porous composite materials by processing cellulose with ionic liquids and supercritical CO. 2 Green Chemistry 10:965. doi:10.1039/b803869d

Uetani K, Izakura S, Kasuga T, Koga H, Nogi M (2018) Self-Alignment Sequence of Colloidal Cellulose Nanofibers Induced by Evaporation from Aqueous Suspensions. Colloids Interfaces 2:71. doi:10.3390/colloids2040071

Varshosaz J, Eskandari S, Tabbakhian M (2012) Freeze-drying of nanostructure lipid carriers by different carbohydrate polymers used as cryoprotectants. Carbohyd Polym 88:1157–1163. doi:10.1016/j.carbpol.2012.01.051

Velásquez-Cock J, Gañán P, Gómez HC, Posada P, Castro C, Dufresne A, Zuluaga R (2018) Improved redispersibility of cellulose nanofibrils in water using maltodextrin as a green, easily removable and non-toxic additive. Food Hydrocolloids 79:30–39. doi:10.1016/j.foodhyd.2017.12.024

Volk N, He R, Magniez K (2015) Enhanced homogeneity and interfacial compatibility in melt-extruded cellulose nano-fibers reinforced polyethylene via surface adsorption of poly(ethylene glycol)- block -poly(ethylene) amphiphiles. Eur Polymer J 72:270–281. doi:10.1016/j.eurpolymj.2015.09.025

Vollick B, Kuo P-Y, Thérien-Aubin H, Yan N, Kumacheva E (2017) Composite Cholesteric Nanocellulose Films with Enhanced Mechanical Properties. Chem Mater 29:789–795. doi:10.1021/acs.chemmater.6b04780

Wang J, Liu X, Jin T, He H, Liu L (2019a) Preparation of nanocellulose and its potential in reinforced composites: A review. J Biomater Sci Polym Ed 30:919–946. doi:10.1080/09205063.2019.1612726

Wang Q, Yao Q, Liu J, Sun J, Zhu Q, Chen H (2019b) Processing nanocellulose to bulk materials:. a review Cellulose 26:7585–7617. doi:10.1007/s10570-019-02642-3

Wang W, Fu S, Leu S-Y, Dong C (2018) A Nano-Ink for gel pens based on scalable. CNC preparation Cellulose 25:6465–6478. doi:10.1007/s10570-018-2036-4

Wu H-F, Brodbelt JS (1994) Gas-Phase Complexation of Monopositive Alkaline Earth Metal Ions with Polyethers: Comparison with Alkali Metal Ion and Aluminum Ion Complexations. J Am Chem Soc 116:6418–6426. doi:10.1021/ja00093a049

Yang M et al (2017) Biomimetic Architectured Graphene Aerogel with Exceptional Strength and Resilience. ACS Nano 11:6817–6824. doi:10.1021/acsnano.7b01815

Yue H, Liu Z (2016) Densities and surface tensions of binary mixtures of biodiesel, diesel, and n-butanol Korean. Journal of Chemical Engineering 33:1692–1697. doi:10.1007/s11814-015-0290-9

Zhang X et al (2019) Redispersibility of cellulose nanoparticles modified by phenyltrimethoxysilane and its application in stabilizing Pickering emulsions. Journal of Materials Science 54:11713–11725. doi:10.1007/s10853-019-03691-6

Zhang X, Xiong R, Kang S, Yang Y, Tsukruk VV (2020) Alternating Stacking of Nanocrystals and Nanofibers into Ultrastrong Chiral Biocomposite Laminates ACS Nano 14 doi:10.1021/acsnano.0c06192

Zheng X, Fu S (2019) Reconstructing micro/nano hierarchical structures particle with nanocellulose for superhydrophobic coatings. Colloids Surf A 560:171–179. doi:10.1016/j.colsurfa.2018.10.005

Zhou Y et al (2019) Methodology of Redispersible Dry Cellulose Nanofibrils Powder Synthesis under Waterless Condition. ACS Sustainable Chemistry Engineering 7:10690–10698. doi:10.1021/acssuschemeng.9b01340

Zhuo X, Liu C, Pan R, Dong X, Li Y (2017) Nanocellulose Mechanically Isolated from Amorpha fruticosa Linn. ACS Sustainable Chemistry Engineering 5:4414–4420. doi:10.1021/acssuschemeng.7b00478

Figures

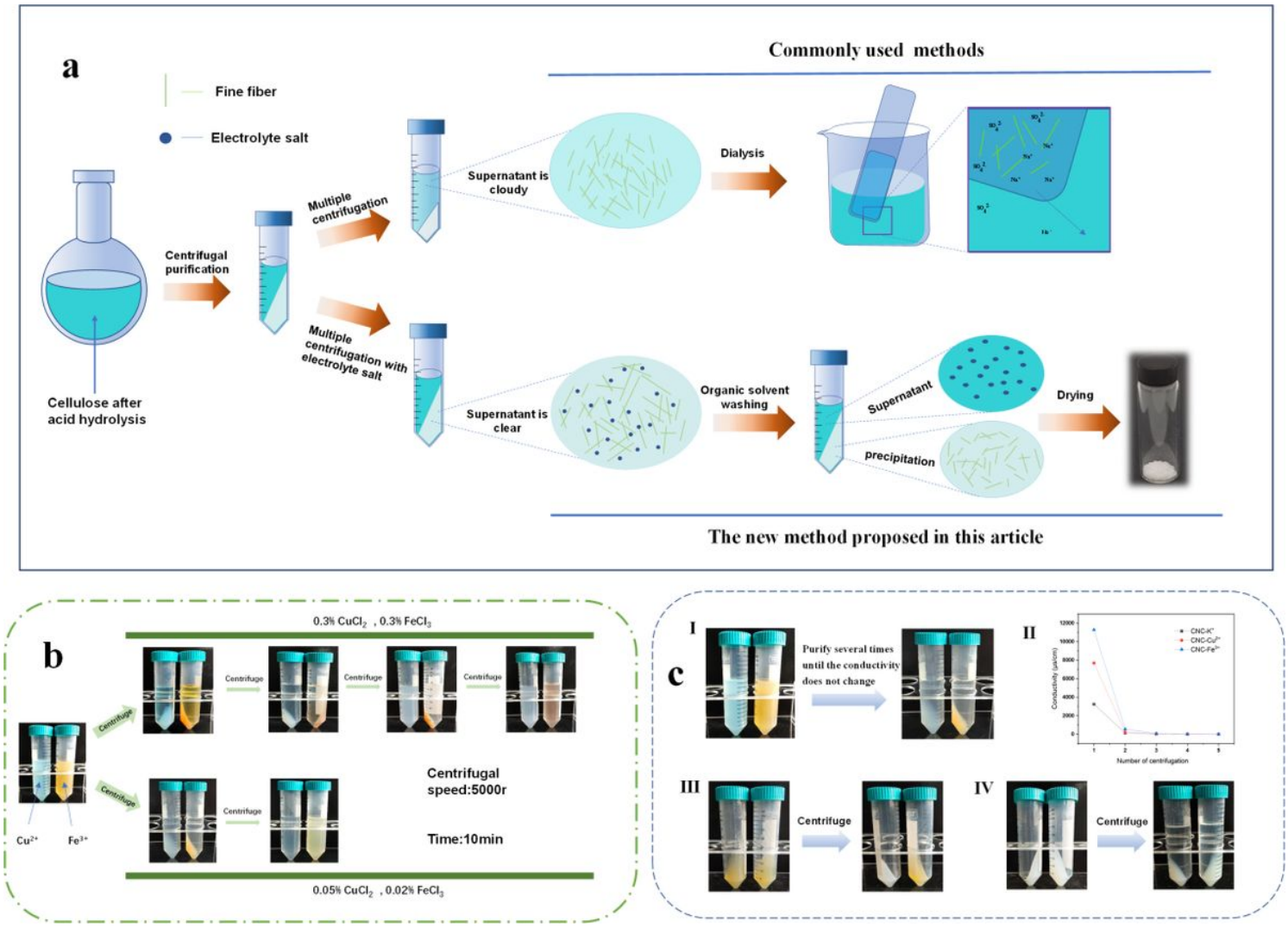

Figure 1

(a) Mechanism diagram of CNC powder preparation (b) Diagram of the agglomeration ability of different valences salts on CNC (c) Schematic diagram of the CNC-metal complex

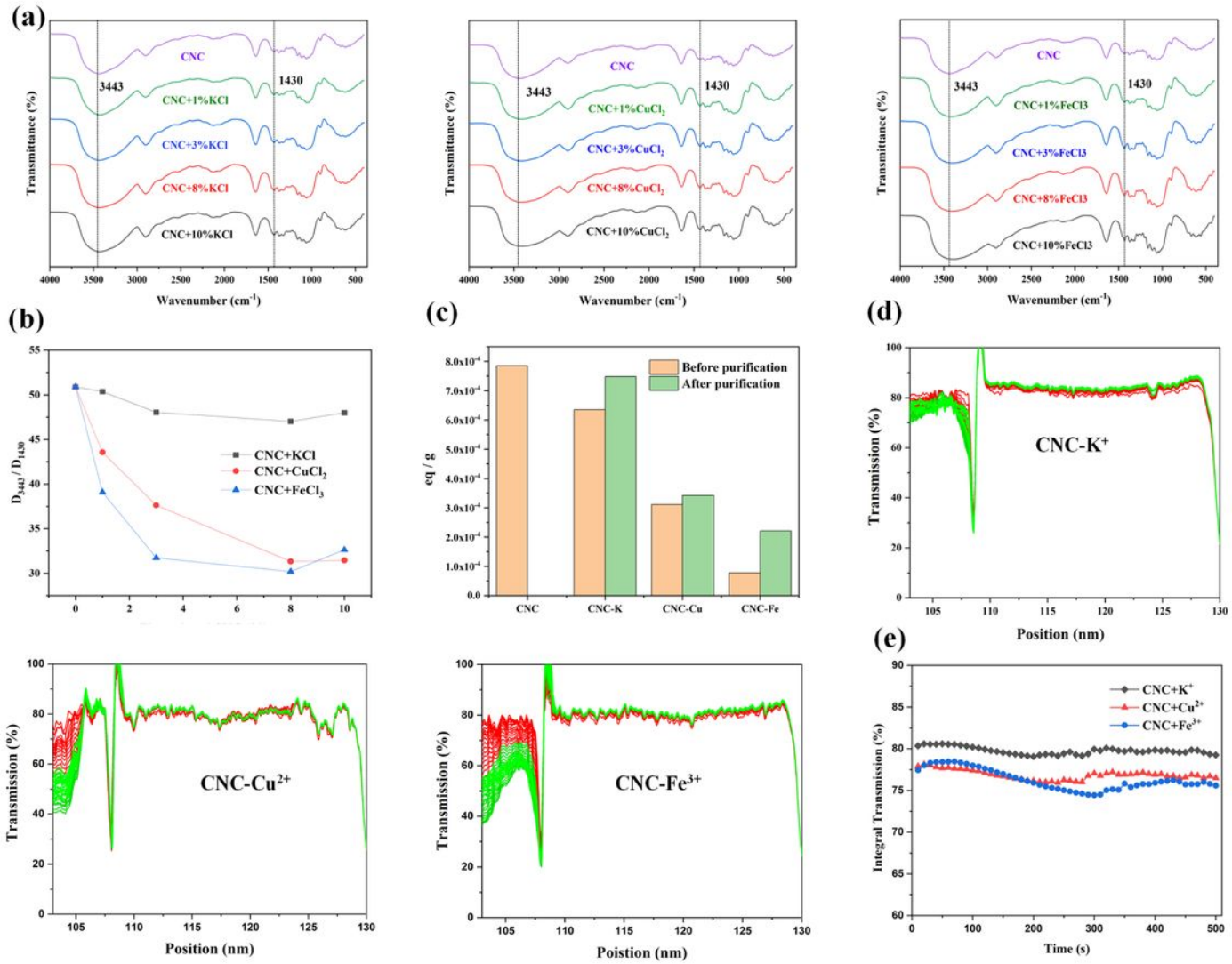

Figure 2

(a) Infrared spectrum of CNC added with different electrolytes (b) Peak area ratio of D3443/D1430 in infrared spectrum (c) Before and after purification, the surface charge of CNC which added with different electrolytes (d) Stability Analyzer profile of CNC-Electrolyte after purification (e) The integral light transmission diagram of the purified CNCs

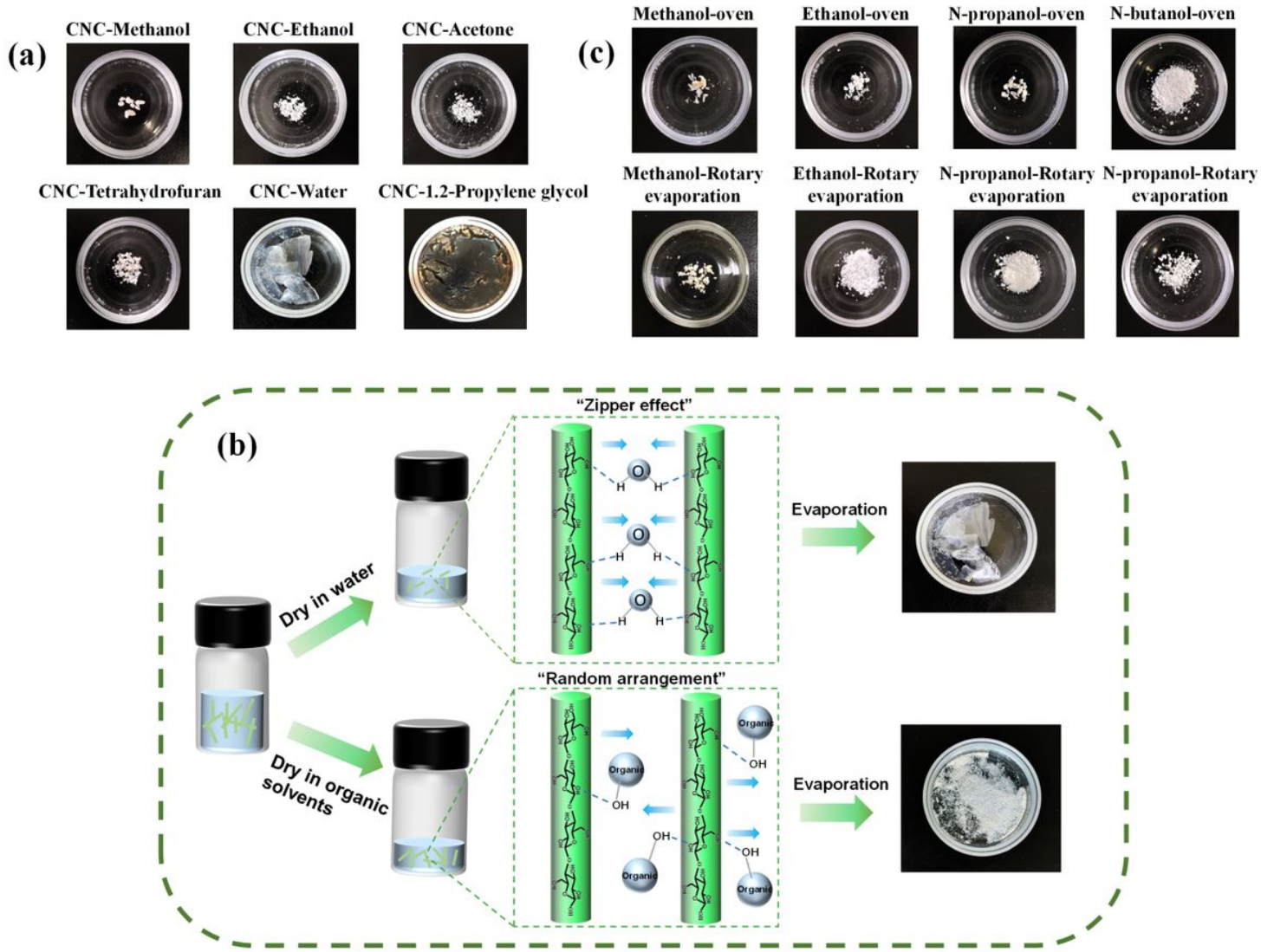

Figure 3

(a) CNC drying in different dispersants (b) Diagram of drying mechanism of different dispersants (c) Dry shape of CNC-organic solvent under different drying conditions

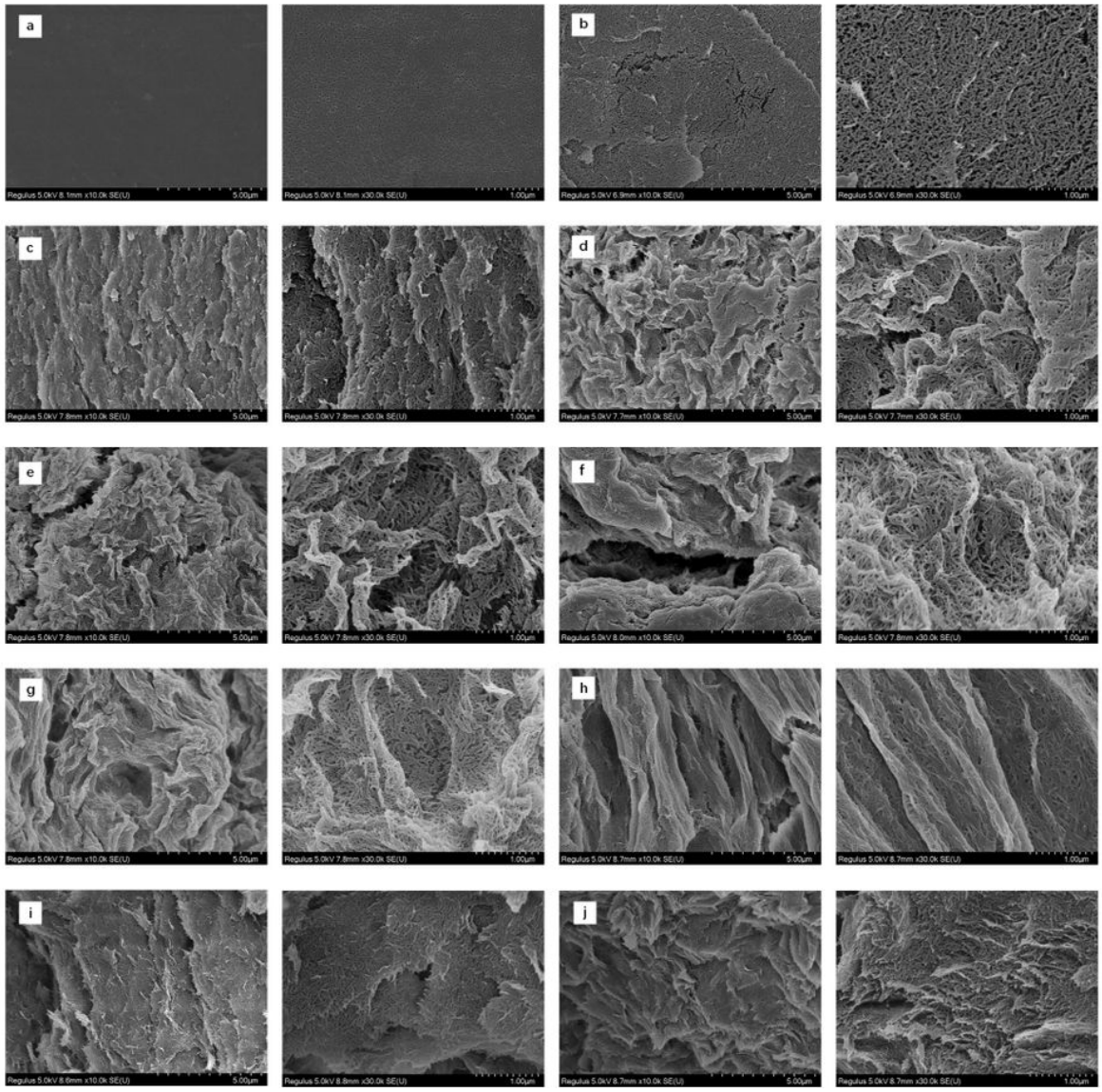

Figure 4

Dry CNCs SEM of (a) CNC-Water (b) CNC-1.2-Propylene glycol (c) CNC-Methanol-Oven (d) CNC-Ethanol-Oven (e) CNC-N-Propanol-Oven (f) CNC-N-Butanol-Oven (g) CNC-Methanol-Rotary Evaporation (h) CNC-Ethanol-Rotary Evaporation (i) CNC-N-Propanol-Rotary Evaporation (j) CNC-Butanol-Rotary Evaporation

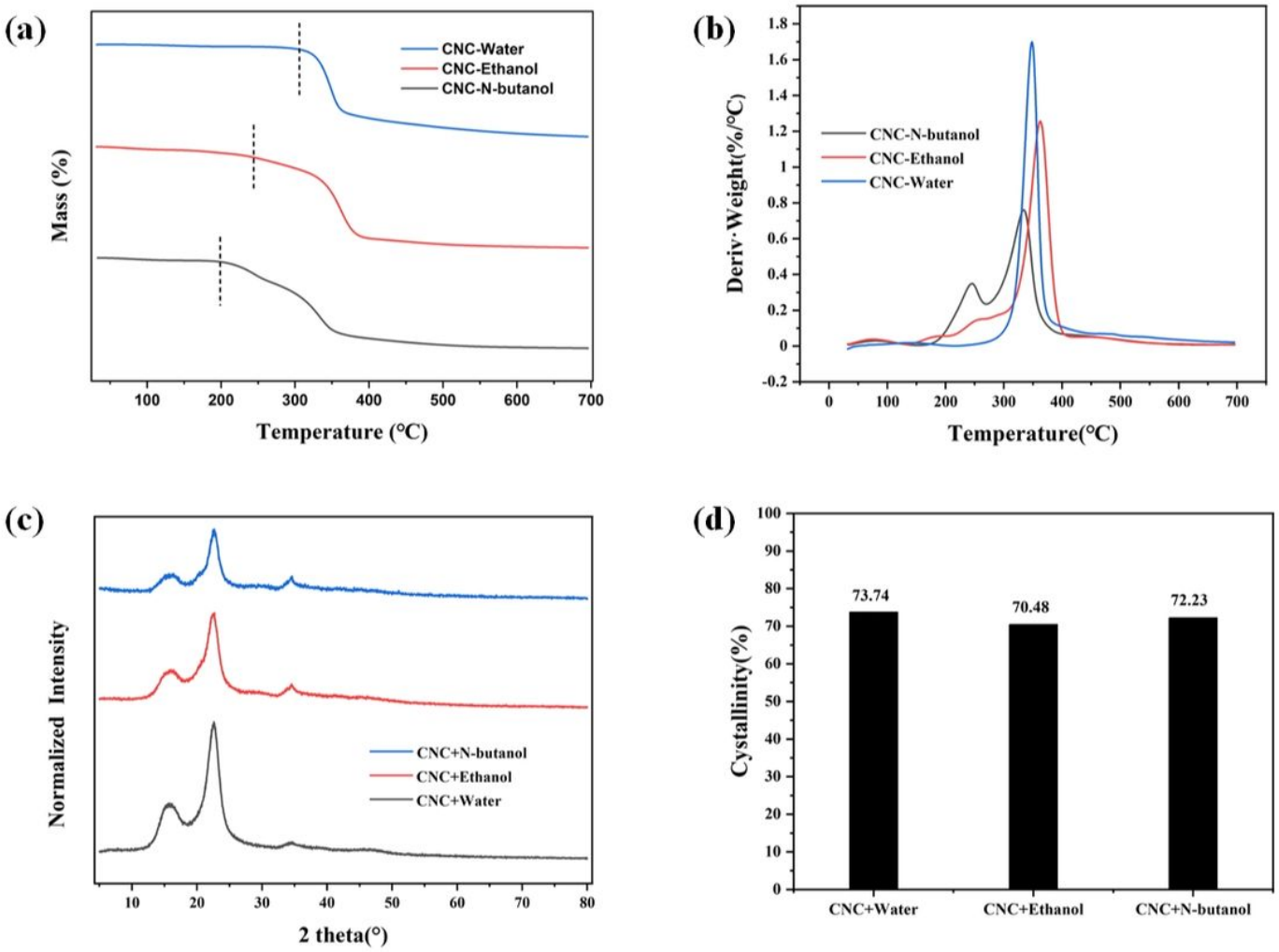

Figure 5

(a) and (b) are thermogravimetry and derivative diagrams of CNC film and CNC powder (c) and (d) are XRD and crystallinity diagrams of CNC film and CNC powder

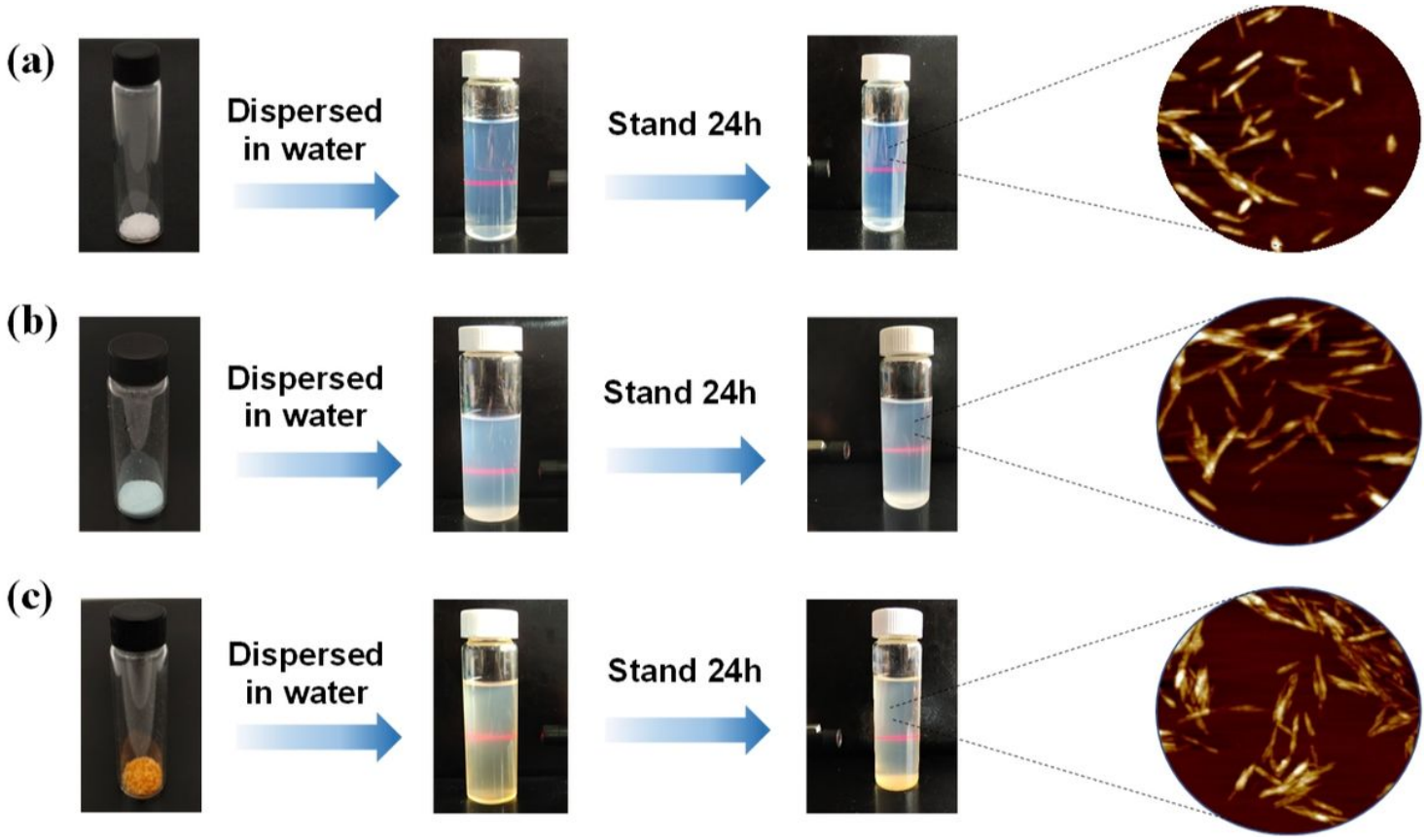

Figure 6

CNC powder re-dispersion diagram (a) CNC-K (b) CNC-Cu (c) CNC-Fe

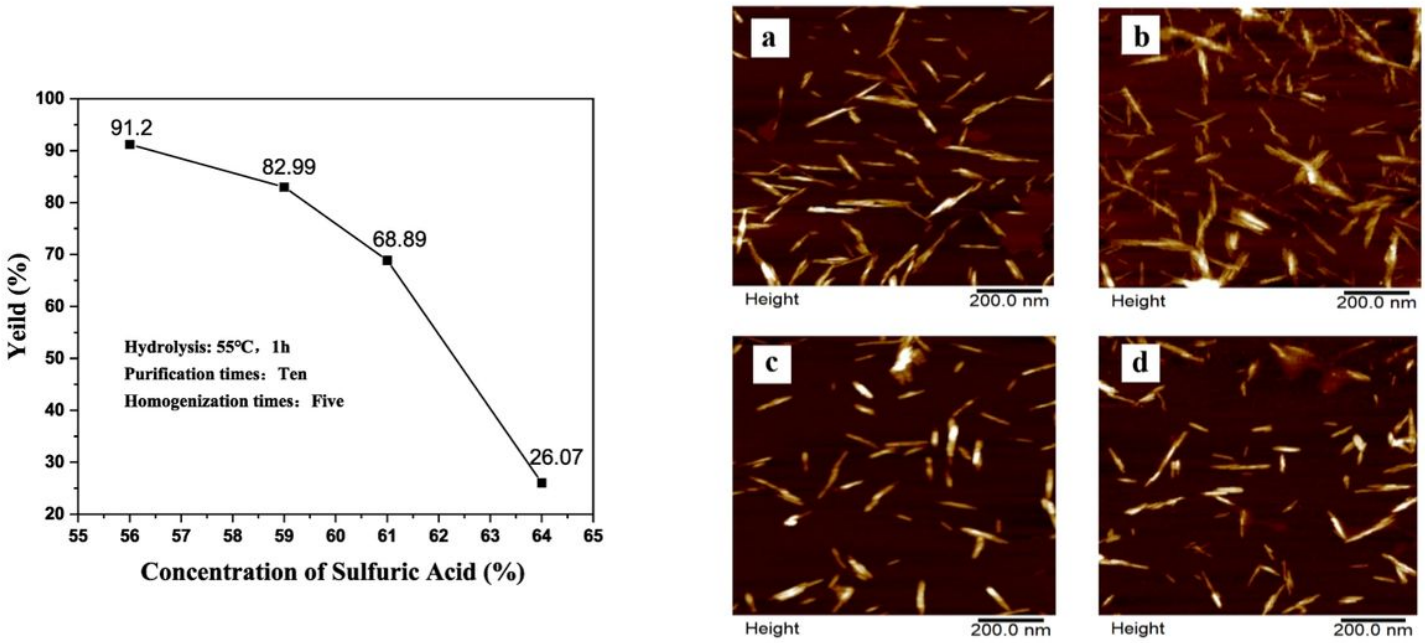

Figure 7

The yield and the AFM diagrams of CNC prepared with four concentrations of sulfuric acid (a) 56wt% (b) 59wt% (c) 61wt% (d) 64wt%

Supplementary Files

This is a list of supplementary files associated with this preprint. Click to download.

- CelluloseSIZhuWang.docx